PERGAMON

Journal of Structural Geology 22 (2000) 1737–1745

JOURNAL OF STRUCTURAL GEOLOGY

www.elsevier.nl/locate/jstrugeo

Fabric anisotropy and its influence on physical weathering of different types of Carrara marbles

Bernd Leiss*, Thomas Weiss

Institute of Geology and Dynamics of the Lithosphere (IGDL), University of Göttingen, Goldschmidtstr. 3, 37077 Göttingen, Germany

Received 10 December 1999; accepted 8 June 2000

Abstract

To evaluate the texture-controlled part on the thermally induced degradation of marbles, the anisotropic thermal dilatation was calculated from texture analyses of four exemplary samples from the Carrara area in Italy and compared to experimentally measured dilatation coefficients. The thermal dilatation as determined in the experiment is controlled by an intrinsic part (anisotropic single crystal properties and texture) and an extrinsic part (e.g. thermally induced microcracks). As expected from theoretical calculations, there is a correlation between the strongest dilatation and the *c*-axis maxima and the weakest dilatation and the *a*-axis maxima according to the single crystal data of calcite. However, a quantitative correlation could not be established. Obviously, other fabric parameters like the grain size, grain shape anisotropies, grain boundary geometries and microcrack formation during heating modify the texture-controlled part significantly. After thermal treatment up to 130°C, all samples show a residual strain. However, the magnitude and directional dependence is remarkably different and is unequivocally correlated to both the microstructure and the texture. Since the number of parameters controlling the physical weathering is very large, a comprehensive quantification of fabrics is indispensible for the understanding of thermally controlled degradation processes of physical weathering in marbles.

1. Introduction and aim of the study

Marbles are widely used as building stones at monuments and statues. Since marbles exhibit a distinct proneness to physical and chemical degradation, the understanding of the weathering processes and mechanisms are of economical and cultural historical interest (Goretzki et al., 1987; Ritter 1992; Trewhitt and Tuchmann, 1988; Grimm, 1999). Besides the local climate, weathering processes and mechanisms of marbles are controlled by the rock's fabric: grain size and grain size distributions, grain shape anisotropies and preferred orientations, grain boundary geometries and crystallographic preferred orientations (texture). Various combinations between these parameters can lead to different properties of the marble types. Thus, a detailed fabric analysis is an appropriate tool for the assessment of marble quality (e.g. Siegesmund et al., 1999).

Since the single crystal of calcite shows a strong anisotropy of the physical properties, theoretically the bulk anisotropies of the physical properties are strongly controlled by the texture (Siegesmund et al., 1997; Leiss and Ullemeyer, 1999; Siegesmund et al., 1999, 2000a). Thus, the question arises if in natural marbles the anisotropic physical properties are really predominantly controlled by the texture or if other microstructural features of the fabric modify or even dominate the texture-controlled proportions. For a first approach, the aim of this study is the comparison between physical properties that are experimentally measured with those calculated from texture measurements. For this aim, this study focuses on the thermal dilatation and the residual strains after thermal treatment as important parameters for the weathering characteristics of marble fabrics. It has been shown in the literature that thermally induced stresses between adjacent grains lead to a decohesion along the grain boundaries (e.g. Frederich and Wong, 1986) and basically all types of marble are degraded after a certain number of thermal cycles even when the heating and cooling is performed carefully (Bertagnini et al., 1984; Franzini, 1995).

2. Sample selection and their macro- and microstructural characterisation

Since historical times, the marbles from the Carrara area in the northern Alpi Apuane in Italy are used as building stones and numerous and spacious quarries are telling from the extensive usage of the material in the past, at present and

* Corresponding author.
E-mail address: bleiss1@gwdg.de (B. Leiss).

0191-8141/00/$ - see front matter
PII: S0191-8141(00)00080-8

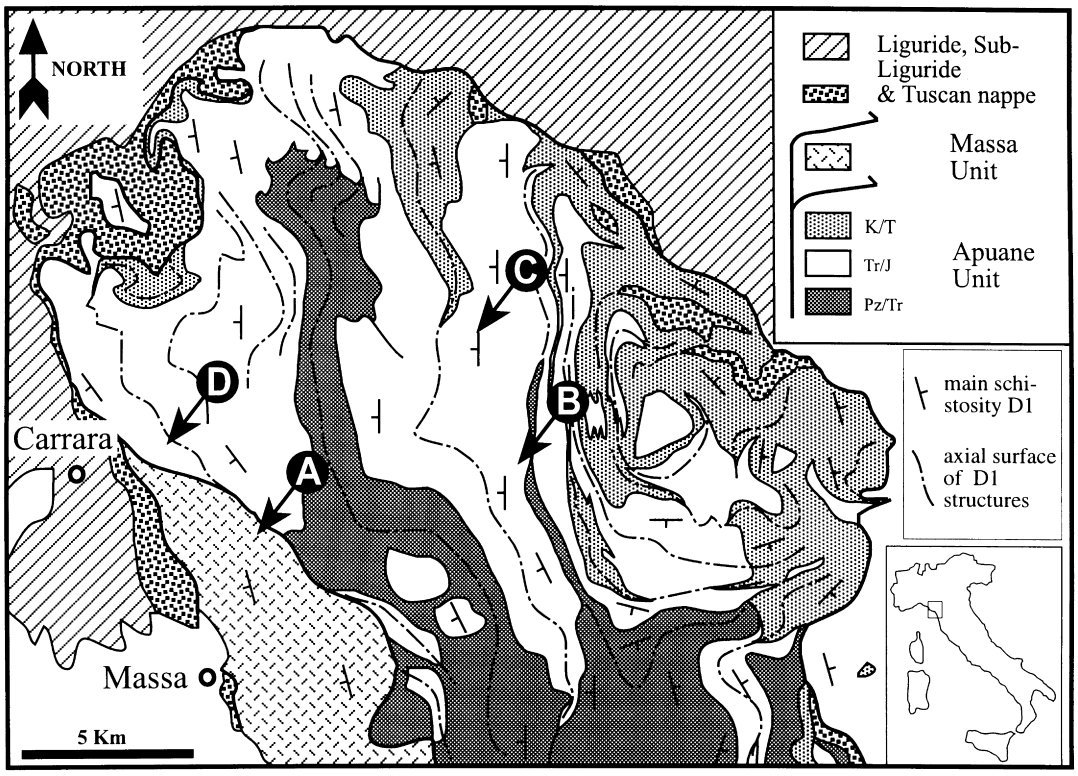

Fig. 1. Geological setting of the Alpi Apuane region with the location of the four samples investigated (A–D). Apuane Unit: Pz//Tr = Paleozoic to Triassic metavolcanics, phyllites, quartzites and metaconglomerates, Tr/J = Upper Triassic to Liassic carbonate platform deposits, K/T = Cretaceous to Tertiary phyllites and metasandstones. Map by courtesey of G. Molli (modified after Carmignani and Kligfield, 1990).

in the future. From this fact, the great interest in the weathering phenomena of especially these marbles is obvious. At the same time, the Carrara marbles are very suitable to the aims of this study because several studies in recent years have shown the large variety of different microstructural features of the Carrara marble fabrics (e.g. Coli, 1989; Barsotelli et al., 1999; Leiss and Molli, 1999; Molli et al., 1999; Oesterling et al., 1999, Rexin et al., 1999; Weiss et al., 1999, Molli et al., 2000). For this study different samples were selected in respect to their significance as case studies for different fabric types. Samples were selected with a large variation in grain size, shape anisotropy, straight/interlobate grain boundaries and texture type and strength. The locations of the four samples selected are indicated in Fig. 1. An *XYZ*-coordinate system was introduced with the following correlation to the macroscopic structural elements: X = parallel to the lineation, Y = normal to the lineation and parallel to the foliation plane, Z = normal to the foliation plane. High polished thin sections were prepared from sections normal to the foliation/parallel to the lineation (*XZ*-plane) and normal to the foliation/normal to the lineation (*XZ*-plane). The grain fabrics of the samples can be macro- and microscopically characterized as follows (compare with Fig. 2):

Sample A comes from the Massa Unit which comprises among others a high-grade metamorphic metasedimentary Middle Triassic to Late Triassic sequence. The sample was collected in the quarries SE of La Rocchetta (South of Colonnata) just above the main thrust between the Massa Unit and the underlaying Apuane Unit (Triassic to Oligocene metasedimentary sequence of low- to medium-grade metamorphsim, Fig. 1). Macroscopic characteristics of the homogenous and white sample are a widely spaced foliation discernible by mica enrichments, a striking SE dipping stretching lineation and a coarse grain size (about 1 mm). Old polished surfaces in the quarry show a remarkable sugar-like degradation, i.e. a decohesion along the grain boundaries. In the section normal to the foliation and parallel to the lineation, the microscopic equigranular fabric exhibits a weak preferred grain shape orientation with a ratio of the short/long axes of up to 1:1.5 (Fig. 2a, left). The grain boundaries are straight to interlobate. Most of the grains are twinned. In the section parallel to the foliation and normal to the lineation, the microstructure is very similar but a grain shape preferred orientation is absent (Fig. 2a, right).

Sample B comes from a hinge zone in the intensively folded area (syncline of Arni) south of Arni (Fig. 1) and is macroscopically a typical representative of the white Carrara marble of the Apuane Unit. Microscopically, the equigranular fabric exhibits a grain size of about 0.5 mm, sutured grain boundaries, no grain shape preferred orientation and an intense twinning (Fig. 2b, left). In the section parallel to the lineation a weak grain shape preferred

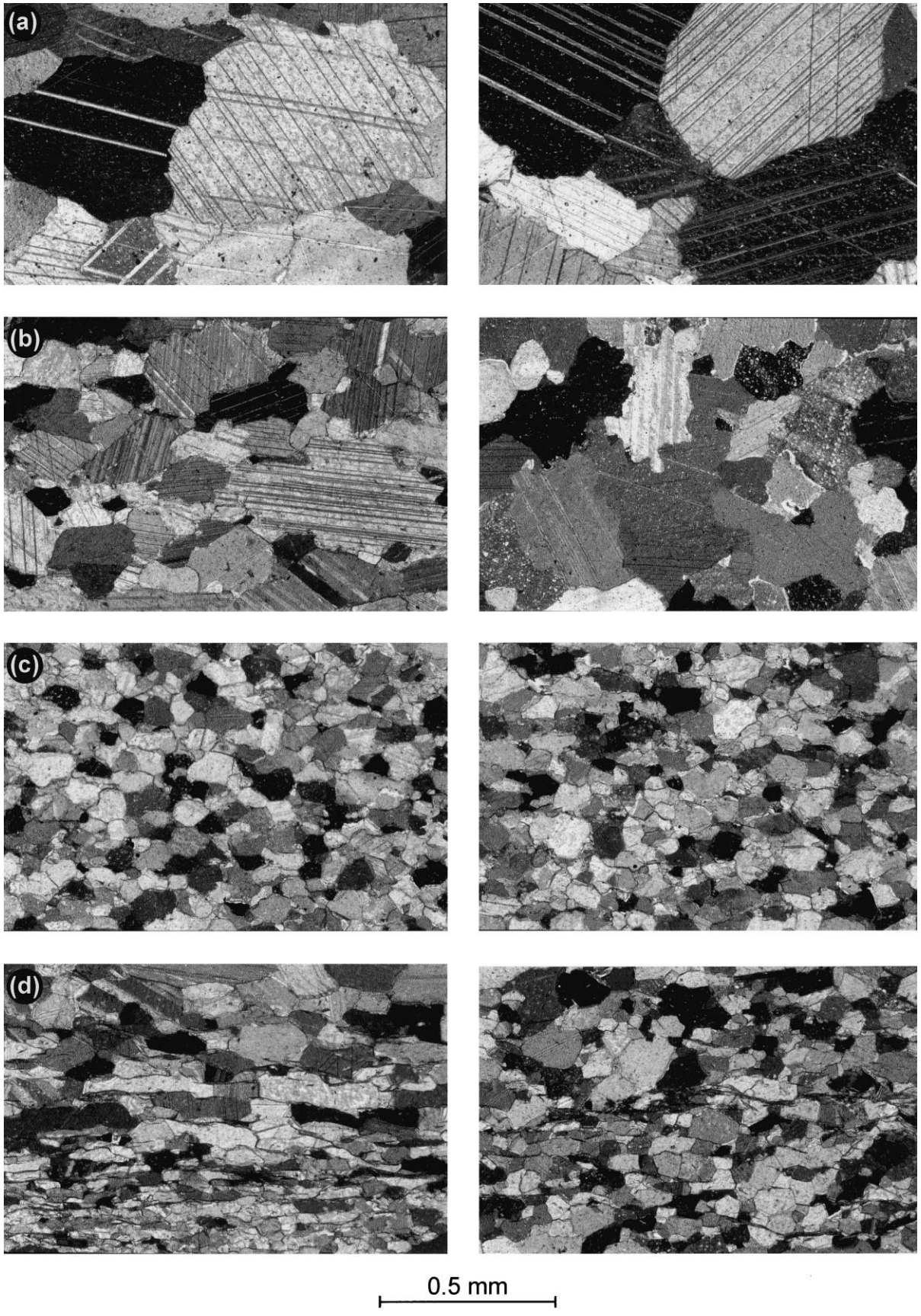

Fig. 2. Photomicrographs of the microstructures (crossed polarizers, same scale for all samples). The microstructures are shown in sections normal to the foliation and parallel to lineation (*XZ*-plane, left row) and normal to the foliation and normal to the lineation (*YZ*-plane, right row) for *Sample A* (a), for *Sample B* (b), for *Sample C* (c) and for *Sample D* (d).

orientation can be observed with long axes parallel to the lineation. In the section normal to the lineation, indications for grain boundary migration are more striking: the grain boundaries are more sutured and more left-over grains can be found (Fig. 2b, right).

Sample C comes from a quarry directly located at the Passo della Focolaccia (North of Resceto, Fig. 1) and also represents a typical marble from the Apuane Unit. The area is a part of the eastern limb of the regional Pianellaccio anticline. A weak stretching lineation is visible on the homogenous, gray and fine-grained (ca. 0.13 mm) sample. The microscopic fabric, however, shows no grain shape anisotropy, but an equigranular grain size distribution and polygonal grain boundaries (Fig. 2c).

Sample *D* comes from the normal limb of the Carrara syncline (Fig. 1). The well-foliated, yellowish sample from the *Z*ebrino levels (Apuane Unit) at the Ponti di Vara (East of Miseglia) shows a prominent grain shape preferred orientation parallel to the lineation with aspect ratios up to 1:10 (Fig. 2d, left). Long axes are ranging from about 0.2 mm in finer grained layers to 2 mm in coarse grained layers. Grain boundaries are straight to curved. Mica layers strengthen the foliation and cleaveage of the sample. In the section normal to the lineation, no grain shape preferred orientation can be observed (Fig. 2d, right).

3. Quantitative analytical methods

3.1. Quantitative texture analysis

To get statistically representative bulk textures and due to the large grain size of most of the samples, neutron diffraction was applied. Measurements were carried out at the SKAT-goniometer at the pulsed reactor IBR-2 in Dubna, Russia (e.g. Ullemeyer et al., 1998; Leiss and Ullemeyer, 1999). From the marbles, spherical samples of a diameter of 30 mm were prepared. A measuring grid of $5° \times 5°$, an exposition time of 15 min per grid point and the application of 19 detectors at the same time resulted in a total measuring time of 18 h. From the time-of-flight spectra, the experimental pole figures of (006), (110), (104), (012) and (113) were extracted. Based on these experimental pole figures, quantitative texture analyses were applied by means of the iterative series-expansion method (Dahms and Bunge, 1989). From the results, pole-figures for the representation (Fig. 3) of the texture and the texture-controlled portions of the anisotropic thermal dilatations were calculated (see also Leiss and Ullemeyer, 1999). The bulk rock anisotropy of the thermal dilatation coefficient was calculated by applying the VOIGT averaging method (e.g. Bunge, 1985) and are represented in stereoplots (Fig. 3).

3.2. Anisotropic thermal dilatation

The measurements of the thermal dilatation were carried out at the Technical University of Vienna. Sample prisms with a size of $10 \times 10 \times 50$ mm were prepared according to the three principal axes of the reference coordinate system (X, Y, Z) given by the structural reference frame (e.g. foliation and lineation, see Fig. 3). The samples were heated in one or more cycles up to a temperature of 130 °C and cooled down to room temperature. Three samples can be measured simultaneously, i.e. under identical experimental conditions (see detailed description in Widhalm et al., 1996). The temperature and the dilatation of the samples were monitored during heating. This allows the calculation of the relative dilatation ε (mm/m) and the thermal dilatation coefficient α (10^{-6} l/°C) as a temperature normalized value (see Fig. 4). A homogeneous heating of the samples was guaranteed by using a slow heating/cooling velocity of 0.75°C/min. Changes in the length of the sample during heating/cooling (dilatation coefficient α) and residual strains after the experiment were measured using linear variable differential transformers (LVDTs). Due to the resolution of the LVTDs, the detection limit is one μm. Since many marbles exhibit residual strains as a consequence of thermally induced microcrack formation in a magnitude of 0.005–0.01 mm after heating, the resolution of these experiments is sufficient to detect thermal degradation of marbles.

4. Results

4.1. Textures

The results of the texture analyses are represented by pole figures in Fig. 3. Textures can be characterized by the intensity of the maximum, by the texture type and by the symmetry. As defined in, e.g. Leiss and Ullemeyer (1999), carbonates form texture types which can be typically lined up in an idealized continous row between a single *c*-axis maximum and an *a*-axes great circle distribution (*c*-axis fibre-type) and a *c*-axis great circle distribution and a single *a*-axis maximum (*a*-axis fibre-type). Refer to Leiss et al. (1994, Fig. 5) and Leiss and Ullemeyer (1999, Fig. 6) for a better understanding of the compatiblity of carbonate pole figures and the modification of the idealized fibre-types by additional texture components.

Sample A shows a relative strong texture and is a typical transition type between the *c*-axis and *a*-axis fibre-type (Fig. 3a). However, features like the intimated *c*-axis girdle, the clearly developed *a*-axis maximum and the small circle distribution of the normals of the *f*-planes around the *a*-axis maximum classifies this texture more as an *a*-axis fibre-type. The *c*-axis maximum is oriented normal to the foliation (*Z*-direction of the coordinate system) and the *a*-axis maximum is oriented parallel to the stretching lineation (*X*-direction of the coordinate system).

Sample B also exhibits a transition type like *Sample A*, but shows a stronger intensity of the *c*-axis maximum. The more distinct *c*-axis maximum and the small circle distributions

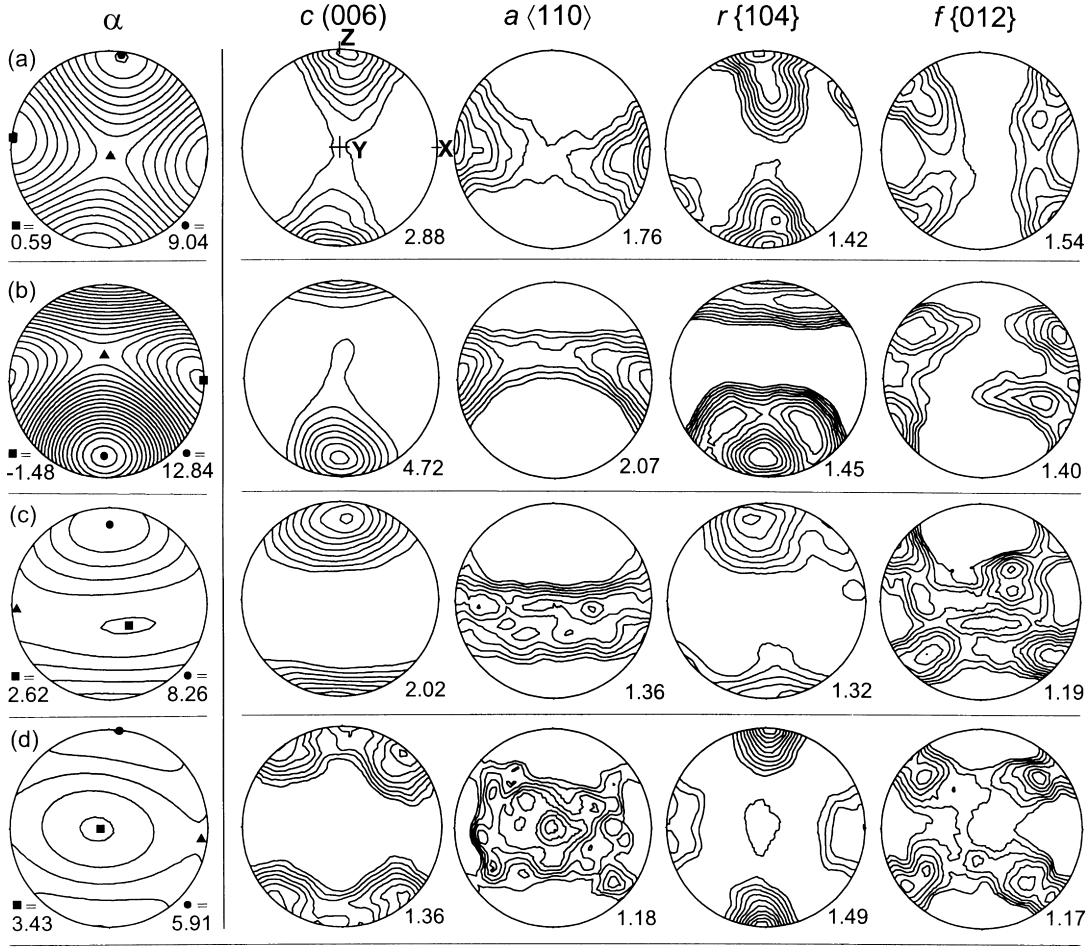

Fig. 3. Textures represented by pole-figures. Pole-figures are calculated from the iterative series expansion method (equal area projection, lowest contour equal to 1.0 multiples of random distribution, relative maxima are given). The left row shows the distribution of the thermal dilatation coefficient α [10^{-6} 1/°C] as calculated from the results of the texture analysis and presented in stereoplots (equal area projection, contour line steps of 0.6 for all plots). Orientations and values of α_{max} (dots) and α_{min} (squares) are indicated in and below the stereoplots; triangles indicate the intermediate values. *X*, *Y*, *Z* indicate the coordinate system, *X* is parallel to the lineation, *Y* is normal to the lineation, parallel to the foliation and the regional fold axes, *Z* is normal to the foliation. The orientation of the pole figures corresponds to the orientation of the photomicrographs in the left row of Fig. 2.

of the normals of the *r*-planes classifies this type more as a *c*-axis fibre-type. The *c*-axis maximum is oriented close to the normal of the axial foliation plane and the *a*-axes are oriented parallel to the fold axis (Fig. 3b).

Sample C can be clearly classified as a *c*-axis fibre-type because the *c*-axis maximum is very clearly developed and the *a*-axes are relatively regularly distributed on a great circle. The *c*-axis maximum is only of moderate intensity and oriented normal to the regional foliation (Fig. 3c).

Sample D shows two conjugate, quite weak but distinct *c*-axis maxima. The *a*-axes pole figure displays not a distinct maximum, but a large and fuzzy area of a weakly developed preferred orientation (Fig. 3d). This classifies the texture as a 'High-Temperature' texture as experimentally developed, e.g. by Kern and Wenk (1983), as predicted by, e.g. Wenk et al. (1986, 1987) by numerical models and as firstly described for a natural sample by Leiss and Molli (1999). The *c*-axis maxima are inclined in respect to the normal of the foliation, the fuzzy area of *a*-axis maxima is oriented normal to the lineation/parallel to the regional fold axes. The symmetry axes of the texture are oriented parallel to *X*, *Y* and *Z*.

4.2. Directional dependence and magnitude of the thermal dilatation

Sample A shows the strongest magnitude of the relative dilatation ε (Fig. 4a). Normal to the foliation the largest dilatation (2.33 mm/m), parallel to the lineation the weakest dilatation can be observed (0.98 mm/m). In contrast, the directional dependence of ε is more pronounced for *Sample B* (Fig. 4b). The strongest dilatation (2.06 mm/m) is found parallel to the *c*-axes maximum and a very weak dilatation (0.24 mm/m) parallel to the *a*-axes maximum. *Sample C* shows a smaller anisotropy of ε varying between 1.92 mm/m parallel to the *c*-axes and 1.15 mm/m parallel to

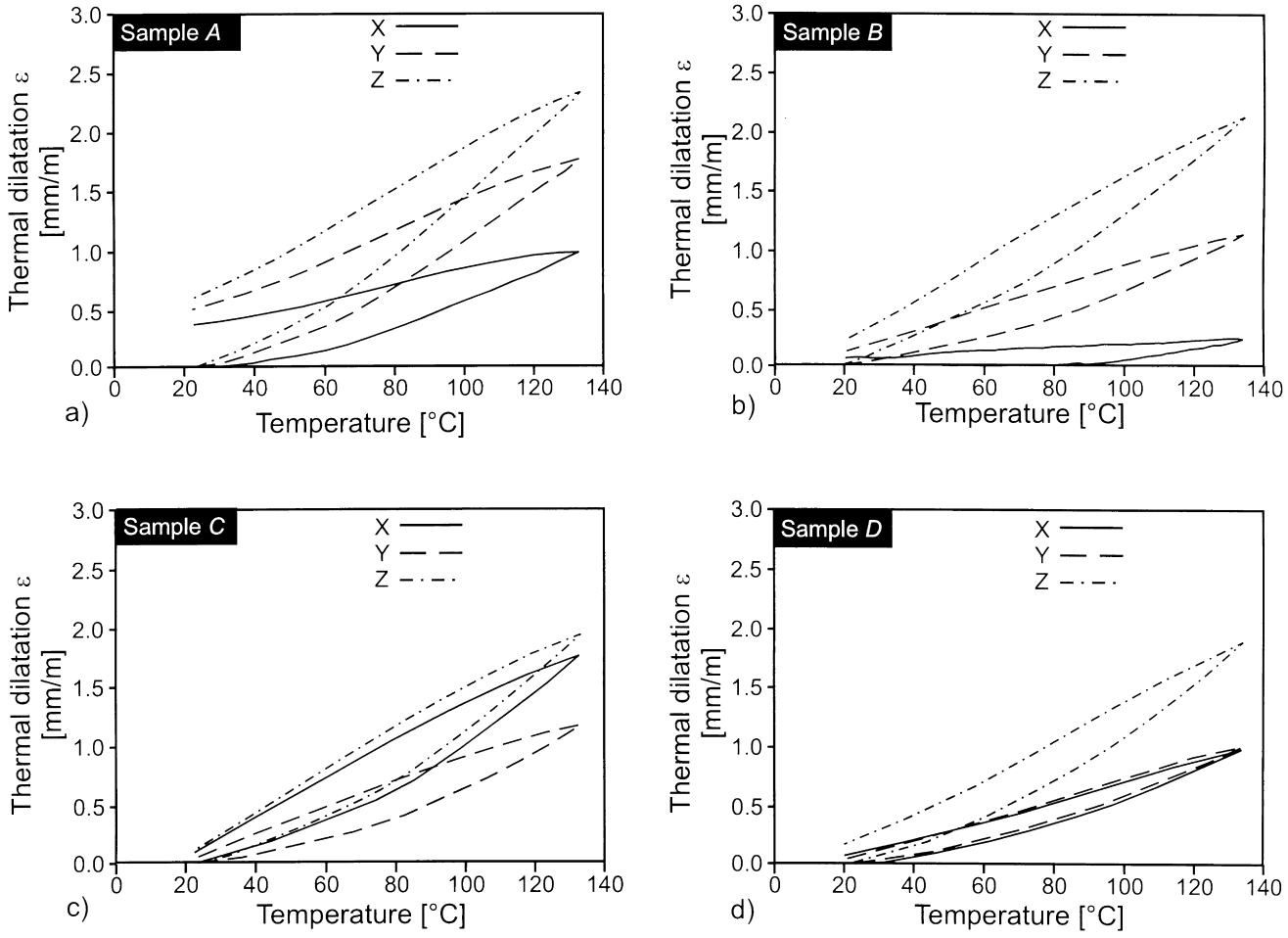

Fig. 4. Directional dependence and magnitude of the thermal dilatation (X = parallel to the lineation = parallel to the a-axis maxima in samples A and B, Y = parallel to the foliation/normal to the lineation, Z = normal to the foliation = parallel to the c-axis maxima in samples A–C).

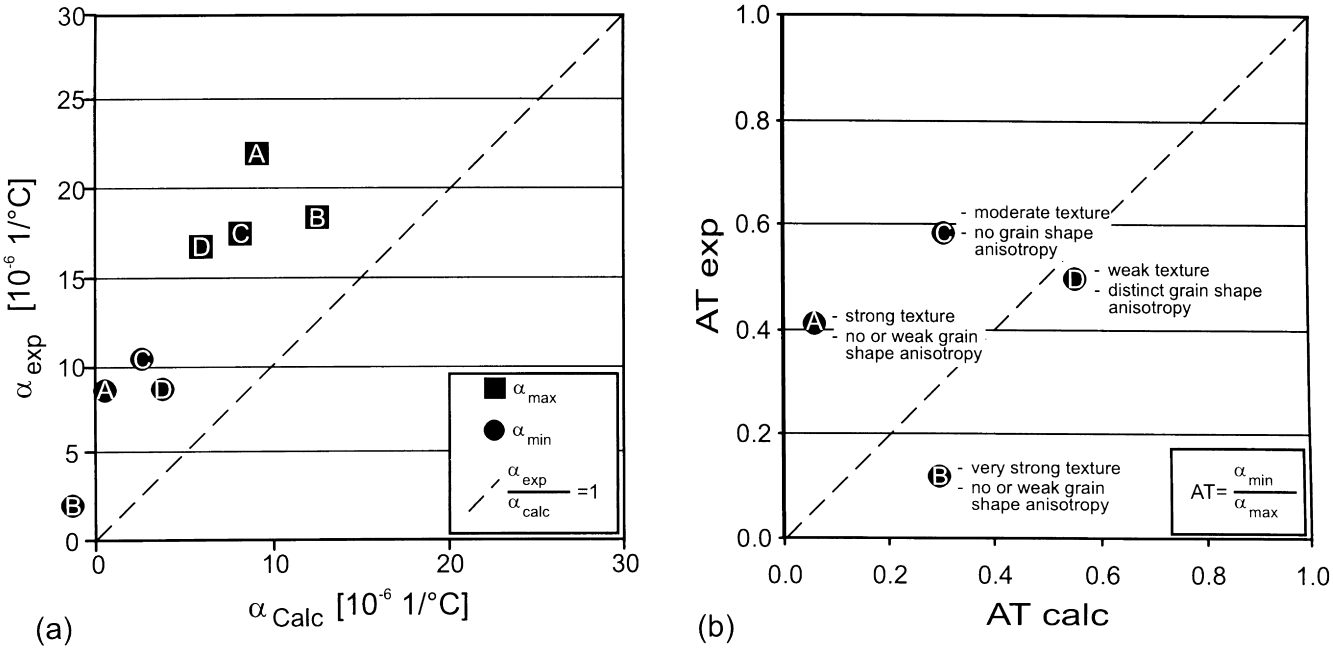

Fig. 5. Thermal dilatation of Carrara marble. (a) α_{max} and α_{min} experimentally determined (α_{exp}) and calculated (α_{calc}). (b) Anisotropy of α (AT) calculated as the quotient of α_{min} divided by α_{max}.

the weak *a*-axis maximum (Fig. 4c). It is conspicuous that despite the well and regular developed *a*-axis girdle, the thermal dilatation ε displays a clear variation in the directions of *X* and *Y*. In *Sample D*, the strongest dilatation (1.90 mm/m) is found normal to the foliation. The weakest dilatations (0.98 mm/m) are observed in the directions of *X* and *Y* and are, in contrast to *Sample C*, very similar (Fig. 4d).

4.3. Residual strain after thermal treatment

A measurable quantity for the thermal degradation of marble is the residual strain after heat treatment (Rosenholtz and Smith, 1949; Franzini, 1995; Widhalm et al., 1996). This thermally induced irreversible change in length can occur even within very small temperature intervals, e.g. after heating samples up to only 50°C (Battaglia et al., 1993). Especially during the first heating cycle, it was observed that all investigated samples show a remarkable non-reversible change in length (Siegesmund et al., 2000b).

Our results (Fig. 4) show that the residual strain and the thermal dilatation ε clearly depend on the direction. Generally, the largest residual strain is observed parallel to the direction of the maximum dilatation ε, i.e. parallel to the *c*-axis maxima. The absolute magnitude of the residual strain, however, is significantly different for the samples. *Sample A* shows relatively large (0.36–0.59 mm/m) residual strains for all directions with the largest residual strain parallel to the *c*-axis maximum. Although the *c*-axis maximum of *Sample B* is stronger and the texture type of *Sample B* is quite similar to *Sample A*, the residual strains for *Sample B* are much smaller for all directions (0.24 mm/m parallel and 0.08 mm/m normal to the *c*-axis maximum). For *Sample C* and *D* the residual strains are quite small (Fig. 3c and d). However, it is striking that the most prominent residual strain can be observed in the direction of *Z* (i.e. normal to the foliation) in *Sample D*, since the *c*-axis maximum and the maximum of the calculated thermal dilatation is much smaller than in *Sample C*.

5. Discussion and conclusions

Model calculations of the thermal dilatation coefficient α on the basis of the texture and the single crystal dilatation data reveal that the directional dependence of the thermal dilation coefficient is clearly controlled by the texture. As from the single crystal data expected, in all samples the strongest dilatation coefficient is found parallel to the *c*-axes maximum and a small dilatation coefficient parallel to the *a*-axes maximum. However, despite a clear variation of the *c*-axes maxima (<1.4–4.72 multiples of random distribution, mrd), the absolute values for the strongest experimentally determined dilatations are very similar (~2.0 mm/m) for all samples. This value is expected for marbles with dilatation coefficients around 19×10^{-6} l/°C and is typical for Carrara marble. Carrara marble is generally assumed to have isotropic physical properties, but the marbles investigated prove a distinct anisotropy which cannot be exclusively explained by the texture. Since the absolute values of the thermal dilatation as well as the anisotropy cannot be directly correlated with the texture, a closer look on additional parameters is required to understand the mechanisms of the degradation in these marbles.

Fig. 5a demonstrates that the experimentally determined thermal dilatation coefficient is generally larger than the one expected from texture calculations (compare Figs. 3 and 4). Using another theoretical model for the calculation of the coefficient like the Reuss method would result in an even larger discrepancy because the here applied Voigt method already holds for the upper bound of the models. A possible explanation for the disrepancy is that during heating a significant amount of thermal stresses in the samples may cause a widening of the pore space or may lead to thermally induced crack nucleation and/or crack growth. Thus, the experimentally observed thermal dilatation is the result of i) an intrinsic part (depending on texture and single crystal constants) and ii) a crack induced part. This crack induced part becomes visible in the measurements (Fig. 4): within the very limited temperature range of the present investigations, the thermal dilatation should be linearly correlated with the temperature. However, especially for *Sample A* and *C* the slope of the curves increases when the sample temperature reaches approximately 60–70°C. This indicates that (i) thermally induced cracks are generated at a certain critical crack initiation temperature or (ii) the total thermal dilatation coefficient is buffered by preexisting crack systems (compare with Weiss et al., 1999) at temperatures lower than about 60°C (Weiss et al., 2000).

A critical parameter for the formation of thermal induced microcracks may be the grain size which can have a profound effect on the rheological behaviour, a fact which is well known from ceramics. Frederich and Wong (1986) found evidence for thermal cracking at 500°C for an untextured limestone with an average grain size of 0.075 mm. Marbles with larger grain sizes show thermal cracking at significantly lower temperatures indicated by an increase of acoustic emissions at temperatures above 50°C (Widhalm et al., 1997). For Al_2O_3 with a thermal dilatation coefficient of 0.5×10^{-6} l/°C, a critical grain-size of 0.4 mm for spontaneous fracturing along grain boundaries was experimentally determined by Rice and Pohonka (1979). Theoretical modeling using an object oriented finite element method reveal that during processing of ceramic materials residual stresses arise high enough to cause spontaneous microcracking (Tschegg et al., 1999). They are the result of thermal dilatation anisotropy of the ceramic material (Vedula et al., 1999). Since the anisotropy of thermal dilatation of calcite is significantly larger than that of Al_2O_3, the critical grain size at which thermal microcracking starts will be significantly smaller (e.g. Evans, 1978). The corresponding thermally-induced crack nucleation starts preferentially at 120° triple points (Evans 1978, Fu and Evans, 1980; Tvergaard and Hutchinson, 1988).

No specific relationship between the *a*-axis maxima (1.2 to 2.1 mrd) and the absolute values of the minimal experimental dilatation (0.2–1.2 mm/m) has been found. This finding additionally supports the idea that the grain size, grain shape and grain boundary geometries are suspected to contribute significantly to the initation of micrcracking and with this to the observed dilatation.

The results do not only indicate the general influence of microcracks on the thermal dilatation, but also give evidence for an anisotropic microcrack distribution. This is especially obvious in *Sample C*. This sample does not display a significant grain shape preferred orientation and shows a very regular distribution of the *a*-axes in the *XY*-plane (Fig. 3). Despite these facts, the dilatation is much stronger in the direction of *X* than in *Y* (compare with *Sample D* where this is not the case). This can be only explained by a much higher microcrack density in the plane normal to *X*. Another good example for a non-uniform crack generation is *Sample D*. Despite the very weak texture, the experimentally determined anisotropy of α in *Z* is as large as in *Sample C* which shows a significantly stronger texture (Fig. 5b). In this case, the anisotropic microcracking must be basically controlled by the strong grain shape anisotropy and the mica layerings. This idea is supported by the following argument: if the elongated grain shape anisotropy would basically control the dilatation, different magnitudes of the dilatation have to be expected for the directions of *X* and *Y*.

An important indicator for the structural disintegration as a result of thermal treatment is the magnitude and directional dependence of the residual strain. The residual strain characterizes the decohesion of the grain boundaries and therefore especially reflects the degree of the durable destruction of the marbles.

Generally, the maximum residual strain is observed in the directions of maximum dilatation. Therefore, the texture is expected to control the residual strain. However, from the comparison of *Samples A* and *B* it becomes obvious that *Sample A* develops a much larger residual strain, despite similar texture and a much weaker anisotropy of the calculated dilatation coefficient of *Sample B* (Figs. 4 and 5b). A much more uniform microcracking in *Sample A* might be responsible for this observation. Due to the relative straight grain boundaries, microcracking seems to be much easier to initiate in *Sample A* than in *Sample B* with its sutured grain boundaries. The obviously more sutured grain boundaries in the section normal to the lineation in *Sample B* might additionally enhance anisotropic microcracking (residual strain is larger in *Z* than in *X* and *Y*). *Sample A* from the Massa Unit shows the most intensive degradation with a residual strain of about 0.6 mm/m. This result matches the observations already made in the field. Compared to the other samples, the most prominent difference of the fabric of this sample is the large grain-size and supports the discussion on the influence of the grain size on the formation of microcracking outlined further above.

6. Summary

Incompatibilities in the correlation of the texture and the experimentally determined thermal dilatation prove that fabric parameters like grain size and grain boundary geometries modify the thermal dilatation properties which are induced by the texture. The modification by, e.g. the grain size and grain boundary geometry works by controlling the initiation of microcracking. For the correlation with the texture and the experimentally determined thermal dilatation/residual strain after heating, more comprising and quantitive analyses of the microstructures are indispensible in order to assess the efficiency of the different parameters involved in the degradation of marble fabrics.

Acknowledgements

We greatly appreciate the field introduction by Giancarlo Molli and the discussions with him. Any discussions with Siegfried Siegesmund are greatly acknowledged. Klaus Ullemeyer is thanked for many helpful discussions on texture analysis and physical properties. The paper has benefitted from the critical comments of Günter Braun and an anonymous reviewer. Technical assistance by Erich Rexin and Heike Gröger is also greatly acknowledged. TW thanks the DFG for a Postdoctoral Fellowship We 2234/1-1 and Prof. Tschegg from the TU Vienna for support of dilatation measurements. This study was financially supported by the german 'Bundesministerium für Bildung und Forschung' (03-DUBGOE1-7) and the Deutsche Bundesstiftung Umwelt (DBU).

References

Barsotelli, M., Fratini, F., Giorgetti, G., Manganelli Del Fà, C., Molli, G., 1999. Microfabric and alteration in Carrara marble: a preliminary study. Science and Technology for Cultural Heritage 7, 115–126.

Battaglia, S., Franzini, M., Mango, F., 1993. High sensitivity apparatus for measuring linear thermal expansion: preliminary results on the response of marbles. Il Nuovo Cimento 16, 453–461.

Bertagnini, A., Franzini, M., Gratziu, C., Spampinato, M., 1984. Il marmo cotto in natura e nei Monumenti. Rend. Soc. It. Miner Petr. 39, 39–46.

Bunge, H.J., 1985. Physical properties of polycrystals. In: Wenk, H.-R. (Ed.), Preferred Orientation in Deformed Metals and Rocks: an Introduction to Modern Texture Analysis. Academic Press, Orlando.

Carmignani and Kligfield, 1990. Crustal extension in the northern Apennines: the transition from compression to extension in the Alpi Apuane core complex. Tectonics 9, 1275–1303.

Coli, M., 1989. Litho-structural assemblage and deformation history of Carrara marble. Bollettino della Societa Geologica Italiana 108, 581–590.

Dahms, M., Bunge, H.-J., 1989. The Iterative Series-Expansion Method for Quantitative Texture Analysis. I. General Outline. Journal of Applied Crystallography 22, 439–447.

Evans, A.G., 1978. Damage and microfracture from thermal expansion anisotropy in polycrystalline ceramics. Acta metallurgica 26, 1845–1853.

Franzini, M., 1995. Stones in monument: natural and anthropogenic

deterioration of marble artifacts. European Journal of Mineralogy 7, 735–743.

Frederich, J.T., Wong T.F., 1986. Micromechanics of thermally induced cracking in three crustal rocks. Journal of Geophysical Research 91, 12, 743–12, 764.

Fu, Y., Evans, A.G., 1980. Some effects of microcracks on the mechanical properties of brittle solids. I: Stress strain relations. Acta metallurgica 33/8, 1515–1523.

Goretzki, L., Füting, M., Köhler, W., 1987. Untersuchungen zur Korrosion der Marmorskulpturen im Park von Potsdam—Sanssouci. Bautenschutz/Bautensanierung 10, 104–109.

Grimm, W., 1999. Beobachtungen und Überlegungen zur Verformung von Marmorprojekten durch Gefügeauflockerung. Zeitschrift der Deutschen Geologischen Gesellschaft 150/2, 195–236.

Kern, H., Wenk, H.-R., 1983. Calcite texture development in experimantally induced ductile shear zones. Contributions to Mineralogy and Petrology 83, 231–236.

Leiss, B., Siegesmund, S., Weber, K., Olesen, N.Ø., 1994. Localized texture components of a naturally deformed dolomite—a contribution to the analysis of texture-forming processes. In: Bunge, H.-J., Siegesmund, S., Skrotzki, W., Weber, K. (Eds.), Textures of Geological Materials. DGM Press, pp. 261–275.

Leiss, B., Molli, G., 1999. Natural 'High-Temperature' Texture in Calcite from the Alpi Apuane, Italy. In: Leiss, B., Ullemeyer, K., Weber, K. (Eds.), Göttinger Arbeiten zur Geologie und Paläontologie SB4 (Textures and Physical Properties of Rocks), pp. 100–101.

Leiss, B., Ullemeyer, K., 1999. Texture characterisation of carbonate rocks and some implications for the modeling of physical anisotropies, derived from idealized texture types. Zeitschrift der Deutschen Geologischen Gesellschaft 150/2, 259–274.

Molli, G., Conti, P., Giorgetti, G., Meccheri, M., Oesterling, N., 1999. Deformation and microfabric development in Carrara marble (Alpi Apuane, Italy). In: Leiss, B., Ullemeyer, K., Weber, K. (Eds.), Göttinger Arbeiten zur Geologie und Paläontologie SB4 (Textures and Physical Properties of Rocks), pp. 129–130.

Molli, G., Conti, P., Giorgetti, G., Meccheri M., Oesterling, N., 2000. Deformation history and microfabric evolution of Alpi Apuane marbles (Carrara Marble), Italy. Journal of Structural Geology 22, 1809–1825.

Oesterling, N., Heilbronner, R., Molli, G., 1999. Textures of calcite-mylonites in Carrara marble—comparison of computer integrated polarization microscopy (CIP) and universal stage-measurements. In: Leiss, B., Ullemeyer, K., Weber, K. (Eds.). Göttinger Arbeiten zur Geologie und Paläontologie SB4 (Textures and Physical Properties of Rocks), pp. 144–145.

Rexin, E., Leiss, B., Molli, G., 1999. Microstructures and textures of the Carrara Syncline/Alpi Apuane, Italy. In: Leiss, B., Ullemeyer, K., Weber, K. (Eds.), Göttinger Arbeiten zur Geologie und Paläontologie SB4 (Textures and Physical Properties of Rocks), pp. 163–165.

Rice, R.W., Pohonka, R.C., 1979. Grain-size dependence of spontaneous cracking in ceramics. Journal of the American Ceramic Society 61, 478–481.

Ritter, H., 1992. Die Marmorplatten sind falsch dimensioniert. Stein 1, 18–19.

Rosenholtz, J.L., Smith, D.Z., 1949. Linear thermal expansion of calcite, var iceland spar and Yule marble. American Mineralogist 34, 846–854.

Siegesmund, S., Vollbrecht, A., Ullemeyer, K., Weiss, T., Sobott, R., 1997. Application of geological fabric analyses for the characterization of natural building stones—case study Kauffung marble. International Journal for Restoration of Buildings and Monuments 3, 269–292.

Siegesmund, S., Weiss, T., Vollbrecht, A., Ullemeyer, K., 1999. Marble as a natural building stone: rock fabrics, physical and mechanical properties. Zeitschrift der Deutschen Geologischen Gesellschaft 150/2, 237–257.

Siegesmund, S., Ullemeyer, K., Weiss, T., Tschegg, E.K, 2000a. Physical weathering of marbles caused by anisotropic thermal expansion. International Journal of Earth Sciences 89, 170–182.

Siegesmund, S., Weiss, T., Tschegg, E.K., 2000b. Control of marble weathering by thermal expansion and rock fabrics. Proceedings of the 9th International Congress of Deterioration and Conservation of Stone 1, 205–214.

Trewhitt, J., Tuchmann, J., 1988. Amoco may replace marble on Chicago headquarters, ENR (March), 11–12.

Tschegg, E.K., Widhalm, C., Eppensteiner, W., 1999. Ursachen mangelnder Formbeständigkeit von Marmorplatten. Zeitschrift der Deutschen Geologischen Gesellschaft 150/2, 283–298.

Tvergaard, V., Hutchinson, J.W., 1988. Microcracking in ceramics induced by thermal expansion or elastic anisotropy. Journal of the American Ceramic Society 71, 157–166.

Ullemeyer, K., Spalthoff, P., Heinitz, J., Isakov, N.N., Nikitin, A.N., Weber, K., 1998. The SKAT texture diffractometer at the pulsed reactor IBR-2 at Dubna: experimental layout and first measurements. Nuclear Instruments & Methods in Physics Research A 412/1, 80–88.

Vedula, V.R., Glass, S.J., Saylor, D.M., Rohrer, G.S., Carter, W.C., 1999. Predicting microstructural-level residual stresses and crack paths in ceramics. In: Szpunar, J.A. (Ed.), Proceedings of the 12th International Conference on Textures of Materials, NRC Research Press, Ottawa, pp. 1502–1592.

Weiss, T., Leiss, B., Oppermann, H., Siegesmund, S., 1999. Microfabric of fresh and weathered marbles: Implications and consequences for the reconstruction of the Marmorpalais Potsdam. Zeitschrift der Deutschen Geologischen Gesellschaft 150/2, 313–332.

Weiss, T., Siegesmund, S., Rasolofosaon, P.N.J., 2000. The relationship between deterioration, fabric, velocity and porosity constraint. Proceedings of the 9th International Congress of Deterioration and Conservation of Stone 1, 215–224.

Wenk, H.R., Takeshita, T., Van Houtte, P., Wagner, F., 1986. Plastic anisotropy and texture development in calcite polycrystals. Journal of Geophysical Research 91, B3, 3861–3869.

Wenk, H.R., Takeshita, T., Bechler, E., Erskine, B.G., Matthies, S., 1987. Pure shear and simple shear on calcite textures. Comparison of experimental, theoretical and natural data. Journal of Structural Geology 9, 731–745.

Widhalm, C., Tschegg, E., Eppensteiner, W., 1996. Anisotropic thermal expansion causes deformation of marble cladding. Journal of Performance of Constructed Facilities, ASCE 10, 5–10.

Widhalm, C., Tschegg, E., Eppensteiner, W., 1997. Acoustic emission and anisotropic expansion when heating marble. Journal of Performance of Constructed Facilities, ASCE 11, 35–40.